Crystals 2022

MDPI

Proceedings

Crystal structures of various perovskite halide compounds expected for solar cells

Takeo Oku*

Department of Materials Science, The University of Shiga Prefecture, 2500 Hassaka, Hikone, Shiga 522-8533, Japan
* Correspondence: oku@mat.usp.ac.jp; Tel.: +81-749-28-8368

Abstract: Crystal structures of various types of perovskite halide compounds expected for solar cells were summarized and described. In addition to the standard 3-dimensional $CH_3NH_3PbI_3$ perovskite compound, other halides such as cation ordered double perovskite compounds and low dimensional perovskites with 2-, 1-, or 0-dimensionalities were described. Atomic arrangements of these perovskite compounds can be investigated by X-ray diffraction, and the X-ray diffraction was calculated and discussed based on the structural model. These results are useful for structure analysis of perovskite halide crystals, which are expected to be next-generation solar cell materials.

Keywords: perovskite; crystal structure; double perovskite; dimensionality; halide; solar cell; low dimensional perovskite

Citation: Lastname, F.; Lastname, F.; Lastname, F. Title. *Chem. Proc.* **2021**, *3*, x. https://doi.org/10.3390/xxxxx

Published: date

1. Introduction

$CH_3NH_3PbI_3$ perovskite compounds had been applied to solar cell materials [1], and the perovskite solar cells have been extensively produced and studied [2]. Subsequently to achievement of conversion efficiency of ~15% [3], higher conversion efficiencies have been reported for a number of varied devices and perovskite halide crystals [4–9], and efficiencies over 25% were achieved [10]. These perovskite solar cells provide high conversion efficiencies and easy fabrication process that are comparable to organic-based solar cells.

The photovoltaic performances of the perovskite solar cells depend on the perovskite halide structures, electron transport layers, hole transport layers, nanoporous scaffold layers, and their interfacial structures. Particularly, atomic structures of the perovskite crystals have an effect upon energy gaps and carrier mobility. The purpose of the present work is to investigate and summarize the crystal structures of various types of perovskite halide compounds such as basic $CH_3NH_3PbI_3$ ($MAPbI_3$), Cs-based halide, element-substituted perovskites, low-dimensional perovskites and double perovskites, which are expected to be usable as photovoltaic device materials.

2. Structures of $CH_3NH_3PbI_3$, Cs-based and elemental substituted perovskites

Presently, $CH_3NH_3PbI_3$ is the most standard and widely used compounds for perovskite solar cells, as shown in Figure 1(a). Although the crystal structure of the $CH_3NH_3PbI_3$ has been investigated in detail, there are still some vague regions, and several structural models are proposed. Detailed crystal systems and lattice constants of $CH_3NH_3PbI_3$ were reported and summarized [11].

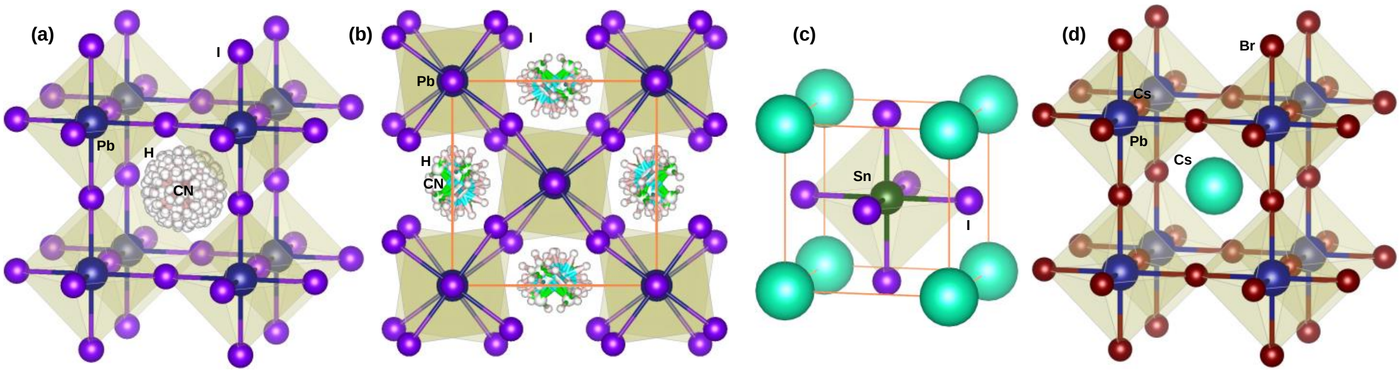

Figure 1. Crystal structures of (c) cubic $CH_3NH_3PbI_3$, tetragonal $CH_3NH_3PbI_3$ (c) $CsSnI_3$, and (d) $CsPbBr_3$.

The $CH_3NH_3PbI_3$ crystals show structural transitions upon heating [12–14]. As the temperature decreases to ~330 K, the cubic phase is transformed into the tetragonal phase [15,16], as shown in Figure 1(b). This transition temperature of ~330 K is nearly room temperature, which may also cause the structural instability. In the actual devices, a very weak reflection corresponding to the tetragonal symmetry may appear, and it might be better to refer to the cubic phase as a "pseudo-cubic" phase, which has nearly cubic symmetry with an a/c ratio of ~1 [11].

Numerous kinds of elemental substituted perovskite halides have been reported [11]. Partial elemental substitutions are often introduced for the $CH_3NH_3PbI_3$ perovskite crystals to control the optoelectronic properties. For example, iodine atoms can be replaced by Br and Cl [17,18]. Examples of elemental substitutions are shown in Figure 1(c) and 1(d). When Pb^{2+} ions are substituted by Sn^{2+} ions, the diffraction intensities of $CH_3NH_3SnI_3$ change compared with those of $CH_3NH_3PbI_3$. $CH_3NH_3^+$ ions can also be substituted by Cs^+ ions, as shown in the structural models of $CsSnI_3$ in Figure 1(c) [19]. When the I^- ions are substituted by Br− ions (Figure 1(d)), the diffraction peaks are shifted to higher angles.

The performances of photovoltaic devices are strongly dependent on the elemental compositions of the perovskite halide crystals. Doping some elements such as tin (Sn) [20], antimony (Sb) [21], copper (Cu) [22–25], arsenic (As) [26], germanium (Ge) [27,28], zinc (Zn) [28,29], indium (In) [30], thallium (Tl) [30], cobalt (Co) [31,32], europium (Eu) [33], or bismuth (Bi) [34] at the lead (Pb) site has been attempted and investigated.

Introducing cesium (Cs) [35,36], rubidium (Rb) [24,37], potassium (K) [38-40], sodium (Na) [23], formamidinium ($HC(NH_2)_2$, FA) [41,42], ethylammonium ($CH_3CH_2NH_3$, EA) [43,44], or guanidinium ($C(NH_2)_3$, GA) [45-47] at the methylammonium (CH_3NH_3, MA) site could also affect the electronic states of the perovskite halides and enhance the conversion efficiencies.

3. Double perovskites and low-dimensional perovskites

As well as the ordinary elemental substitution, atomic orderings of the substituted elements have also been achieved and reported, which is called double perovskite or elpasolite. The general formula is $A_2BB'X_6$, and the ionic valence of B/B′ is $1^+/3^+$ or $2^+/2^+$. One of the examples of the double perovskite structure is $Cs_2AgBiBr_6$, and the structural model is shown in Figure 2(a) [11]. $AgBr_6$ and $BiBr_6$ octahedra are alternately ordered in the perovskite crystal, as shown in Figure 2(a).

Various double perovskite halide compounds such as $Cs_2NaBiCl_6$, Cs_2KEuCl_6, $Cs_2LiScCl_6$, $(CH_3NH_3)_2AgBiBr_6$, $Rb_2NaCrCl_6$, and others have been reported and summarized [11], which are all Pb-free compounds. A calculated X-ray diffraction pattern of $Cs_2AgBiBr_6$ is shown in Figure 3. Peak intensities are fairly different from the standard $MAPbI_3$, and the peaks were shifted to higher or lower angles by substituting elements. Some of these double perovskite elpasolite compounds are expected to apply to Pb-free solar cells [48,49], and the energy gaps have been reported [50].

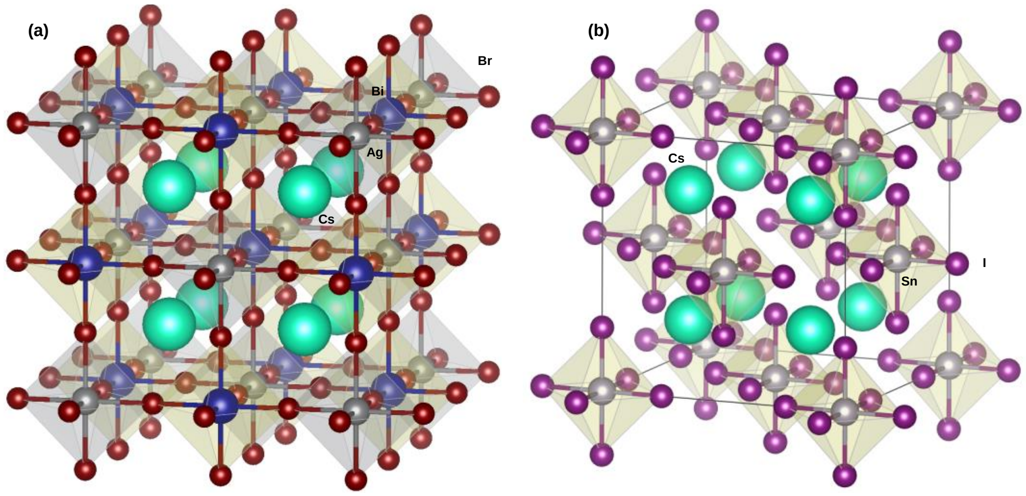

Figure 2. Crystal structures of (a) $Cs_2AgBiBr_6$ double perovskite and (b) 0D Cs_2SnI_6.

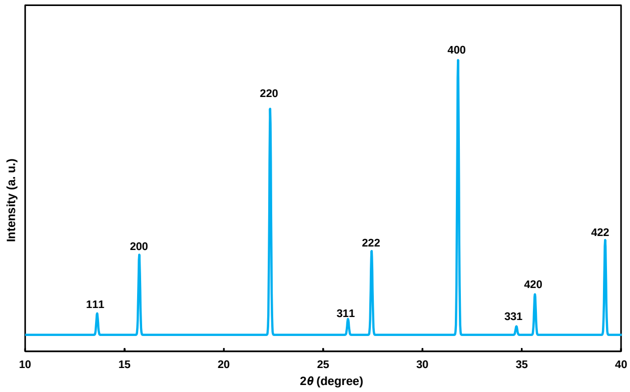

Figure 3. Calculated XRD pattern of $Cs_2AgBiBr_6$ double perovskite.

For the device conformation, highly crystalline-orientated grains and dendritic structures can be formed and affected the photovoltaic properties. The actual crystal structures of perovskite halides in the thin film configuration can be investigated by Rietveld analysis optimizing the atomic coordinates and occupancies [11,51].

Application of the double perovskite elpasolites are also be expected for thermal neutron scintillator materials [52]. Other types of double perovskite compounds such as vacancy-ordered double perovskites and 2-dimensional double perovskites have also been reported.

Normal perovskite halide compounds, as described in the section 2, consist of octahedra sharing all vertices with the neighboring octahedra 3-dimensionally. In addition to the common 3-dimensional (3D) perovskites, various perovskite compounds with lower dimensional structures have been reported [11,53]. Like 2-dimensional (2D) superconducting copper oxide perovskites [54,55], the derivative structures with lower dimensionality could provide finer tunability of the electronic properties [56].

For the 0-dimensional (0D) perovskite, all BX_6 octahedra are isolated in the perovskite crystal, as shown in Figures 2(b) [11]. For the Cs_2SnI_6 compound in Figure 2(b), there are insufficient Sn atoms to form $CsSn_{0.5}I_3$, and the SnI_6 octahedra are isolated in the crystal with A site cations occupying the cuboctahedral voids. From the viewpoint of double perovskites, elements with tetravalent cations are incorporated to form $4^+/0$ double perovskites. This is called vacancy-ordered double perovskites with the general formula of A_2BvX_6, where the v means vacant positions corresponding to the B′ site for the $A_2BB'X_6$ double perovskites. Despite the isolated octahedral BX_6 units, the close-packed iodide lattice provides electronic dispersion, and Cs_2SnI_6 and other perovskites were applied to solar cells [57,58]. Pb free solar cells such as $FA_4GeSbCl_{12}$ have been reported [59], in which the double elements were selected to replace Pb. $Cs_2TiI_xBr_{6-x}$ vacancy-ordered double perovskite compounds were also reported to have stability and bandgaps between 1.0 and 1.8 eV [60].

In addition to the 3D and 0D perovskite compounds, 1-dimensional (1D) continuously connected octahedra exist in $CsTiCl_3$ and $Cs_3Sb_2Cl_9$. $MA_2CuCl_xBr_{4-x}$ were also synthesized as Pb-free light harvesters [61,62] with two-dimensionality (2D). Other types of 2D layered perovskites were also reported, which is called the Dion-Jacobson (DJ) structure [63], which. The lead iodides with DJ perovskite structures have the standard formula of $A(MA)_{n-1}Pb_nI_{3n+1}$. Ruddlesden-Popper 2D perovskite structures were also reported [64]. These perovskite compounds consist of inorganic perovskite layers inserted with butylammonium cations.

In addition to the above 2D perovskites, 2D double perovskite halides such as $PA_4AgBiBr_8$ and $PA_4AgInCl_8$ were synthesized by incorporating organic spacer cations such as propylammonium and octylammonium into standard 3D double perovskites [65]. The band gap energy can be tuned by selecting the spacer layer thickness [50, 65]. First principle calculations will also predict the properties and stabilities of the perovskite structures [66,67].

4. Conclusion

Several types of element substituted perovskite and double perovskite halides were described. Cation- or vacancy-ordered double perovskite compounds could be the one of the candidates for Pb-free perovskite solar cells. Low dimensional perovskite compounds with 2-, 1-, or 0-dimensionality and 2-dimensional double perovskites were also described, which will provide the further diversity of these perovskite halides. Even for the single crystal of $MAPbI_3$, some amounts of defects such as CH_3NH_3 could exist, and the electronically neutral conditions may be maintained by the iodine defects or mixed cation valences of Pb^{2+} and Pb^{4+}. This kind of tolerance for defects and nonstoichiometry would provide a wide processing window for these perovskite thin films which could be used for solar cells.

Author Contributions: Conceptualization, T.O.; Methodology, T.O; Formal Analysis, T.O; Data Curation, T.O.; Writing—Original Draft Preparation, T.O.; Project Administration, T.O.; Funding Acquisition, T.O.

Funding: This research was partly funded by a Grant-in-Aid for Scientific Research (C) 21K04809.
Conflicts of Interest: The authors declare no conflicts of interest.

References

1. Kojima, A.; Teshima, K.; Shirai, Y.; Miyasaka, T. Organometal halide perovskites as visible-light sensitizers for photovoltaic cells. *J. Am. Chem. Soc.* **2009**, *131*, 6050–6051, doi:10.1021/ja809598r.
2. Kim, H.-S.; Lee, C.-R.; Im, J.-H.; Lee, K.-B.; Moehl, T.; Marchioro, A.; Moon, S.-J.; Yum, J.-H.; Humphry-Baker, R.; Moser, J.E.; Grätzel, M.; Park, N.-G. Lead iodide perovskite sensitized all-solid-state submicron thin film mesoscopic solar cell with efficiency exceeding 9%. *Sci. Rep*. **2012**, *2*, 591, doi:10.1038/srep00591.
3. Burschka, J.; Pellet, N.; Moon, S.-J.; Humphry-Baker, R.; Gao, P.; Nazeeruddin, M.K.; Grätzel, M. Sequential deposition as a route to high-performance perovskite-sensitized solar cells. *Nature* **2013**, *499*, 316–320. doi:10.1038/nature12340.
4. Bi, D.; Yi, C.; Luo, J.; Decoppet, J.D.; Zhang, F.; Zakeeruddin, S.M.; Li, X.; Hagfeldt, A.; Gratzel, M. Polymer-templated nucleation and crystal growth of perovskite films for solar cells with efficiency greater than 21%. *Nat. Energy* **2016**, *1*, 16142, doi:10.1038/nenergy.2016.142.
5. Jodlowski, A.D.; Roldán-Carmona, C.; Grancini, G.; Salado, M.; Ralaiarisoa, M.; Ahmad, S.; Koch, N.; Camacho, L.; Miguel, G.; Nazeeruddin, M. Large guanidinium cation mixed with methylammonium in lead iodide perovskites for 19% efficient solar cells. *Nat. Energy* **2017**, *2*, 972–979, doi:10.1038/s41560-017-0054-3.
6. Gedamu, D.; Asuo, I.M.; Benetti, D.; Basti, M.; Ka, I.; Cloutier, S.G.; Rosei, F.; Nechache, R. Solvent-antisolvent ambient processed large grain size perovskite thin films for high-performance solar cells. *Sci. Rep.* **2018**, *8*, 12885, doi:10.1038/s41598-018-31184-0.

7. Han, T.H.; Lee, J.W.; Choi, C.; Tan, S.; Lee, C.; Zhao, Y.; Dai, Z.; Marco, N.D.; Lee, S.J.; Bae, S.H.; et al. Perovskite-polymer composite cross-linker approach for highly-stable and efficient perovskite solar cells. *Nat. Commun.* **2019**, *10*, 520–1–10, doi:10.1038/s41467-019-08455-z.
8. Wang, F.; Yang, M.; Yang, S.; Qu, X.; Yang, L.; Fan, L.; Yang, J.; Rosei, F. Iodine-assisted antisolvent engineering for stable perovskite solar cells with efficiency >21.3 %. *Nano Energy* **2020**, *67*, 104224, doi:10.1016/j.nanoen.2019.104224.
9. Mingyu, J.; Choi, I.W.; Go, E.M.; Cho, Y.; Kim, M.; Byongkyu, L.; Seonghun, J.; Yimhyun, J.; Choi, H.W.; Lee, J.; et al. Stable perovskite solar cells with efficiency exceeding 24.8% and 0.3-V voltage loss. *Science* **2020**, *369*, 1615–1620, doi:10.1126/science.abb7167.
10. Kim, G.; Min, H.; Lee, S. K.; Lee, Y. D.; Yoon, M. S.; Seok, I. S. Impact of strain relaxation on performance of α-formamidinium lead iodide perovskite solar cells. *Science* **2020**, *370*, 108, doi:10.1126/science.abc4417.
11. Oku, T. Crystal structures of perovskite halide compounds used for solar cells. *Rev. Adv. Mater. Sci.* **2020**, *59*, 264–305, doi:10.1515/rams-2020-0015.
12. Weber, D. Z. $CH_3NH_3PbX_3$, a Pb(II)-system with cubic perovskite structure. *Z. Naturforschung B*, **1978,** *33*, 1443–1445, doi:10.1515/znb-1978-1214.
13. Poglitsch, A.; Weber, D. Dynamic disorder in methylammoniumtrihalogenoplumbates (II) observed by millimeter-wave spectroscopy. J. Chem. Phys. **1987**, *87*, 6373–6378, doi:10.1063/1.453467.
14. Onoda-Yamamuro,; T. Matsuo, N.; Suga, H. Calorimetric and IR spectroscopic studies of phase transitions in methylammoniumtrihalogenoplumbates (II). *J. Phys. Chem. Solids* **1990**, *51*, 1383–1395, doi:10.1016/0022-3697(90)90021-7.
15. Kawamura, Y.; Mashiyama, H.; Hasebe, K. Structural study on cubic–tetragonal transition of $CH_3NH_3PbI_3$. *J. Phys. Soc. Jpn.* **2002**, *71*, 1694–1697, doi:10.1143/jpsj.71.1694.
16. Baikie, T., Fang, Y.; Kadro, J. M.; Schreyer, M.; Wei, F.; Mhaisalkar, S. G. et al. Synthesis and crystal chemistry of the hybrid perovskite $(CH_3NH_3)PbI_3$ for solid-state sensitised solar cell applications. *J. Mater. Chem. A* **2013**, *1*, 5628–5641. doi:10.1039/C3TA10518K.
17. Suzuki A.; Taguchi M.; Oku T.; Okita M.; Minami S.; Fukunishi S.; Tachikawa T., Additive effects of methyl ammonium bromide or formamidinium bromide in methylammonium lead iodide perovskite solar cells using decaphenylcyclopentasilane, *J. Mater. Sci.: Mater. Electron.* **2021**, *32*, 26449–26464. doi.10.1007/s10854-021-07023-w.
18. Suzuki A.; Kato M.; Ueoka N.; Oku T., Additive effect of formamidinium chloride in methylammonium lead halide compound-based perovskite solar cells, *J. Electron. Mater.* **2019**, *48*, 3900-3907. doi:10.1007/s11664-019-07153-2.
19. Chung, I.; Song, J. H.; Im, J.; Androulakis, J.; Malliakas, C. D.; Li, H. $CsSnI_3$: Semiconductor or metal? High electrical conductivity and strong near-infrared photoluminescence from a single material. High hole mobility and phase-transitions. *J. Am. Chem. Soc.* **2012,** *134*, 8579–8587. doi.org/10.1021/ja301539s.
20. Tavakoli, M. M., Zakeeruddin, S. M.; Grätzel, M.; Fan, Z. Large grain tin-rich perovskite films for efficient solar cells via metal alloying technique. *Adv. Mater.* **2018,** *30*, 1705998. doi:10.1002/adma.201705998.
21. Oku, T., Ohishi, Y.; Suzuki, A. Effects of antimony addition to perovskite-type $CH_3NH_3PbI_3$ photovoltaic devices. Chem. Lett. **2016,** *45*, 134–136. doi:10.1246/cl.150984.
22. Ueoka N.; Oku T.; Suzuki A., Additive effects of alkali metals on Cu-modified $CH_3NH_3PbI_{3-\delta}Cl_\delta$ photovoltaic devices, *RSC Adv.* **2019**, *9*, 24231. doi:10.1039/c9ra03068a.
23. Ueoka, N.; Oku, T. Effects of co-addition of sodium chloride and copper(II) bromide to mixed-cation mixed-halide perovskite photovoltaic devices. *ACS Appl. Energy Mater.* **2020**, *3*, 7272–7283, doi:10.1021/acsaem.0c00182.
24. Ueoka, N.; Oku, T.; Suzuki, A. Effects of doping with Na, K, Rb, and formamidinium cations on $(CH_3NH_3)_{0.99}Rb_{0.01}Pb_{0.99}Cu_{0.01}I_{3-x}(Cl, Br)_x$ perovskite photovoltaic cells. *AIP Adv.* **2020**, *10*, 125023, doi:10.1063/5.0029162.
25. Suzuki A.; Kitagawa K.; Oku T.; Okita M.; Fukunishi S.; Tachikawa T., Additive effects of copper and alkali metal halides into methylammonium lead iodide perovskite solar cells, *Electron. Mater. Lett.* **2021**, doi:10.1007/s13391-021-00325-5.
26. Hamatani, T.; Oku, T. Effects of halide addition to arsenic doped perovskite photovoltaic devices. *AIP Conf. Proc.* **2018,** *1929*, 020018. doi:10.1063/1.5021931.
27. Krishnamoorthy, T.; Ding, H.; Yan, C.; Leong, W. L.; Baikie, T.; Zhang, Z. et al. Lead-free germanium iodide perovskite materials for photovoltaic applications. *J. Mater. Chem. A* **2015**, *3*, 23829–23832. doi:10.1039/C5TA05741H.
28. Tanaka, H.; Ohishi, Y.; Oku, T. Effects of GeI_2 or ZnI_2 addition to perovskite $CH_3NH_3PbI_3$ photovoltaic devices. *AIP Conf. Proc.* **2018,** *1929*, 020007, doi:org/10.1063/1.502192.
29. Zheng, H.; Liu, G.; Xu, X.; Alsaedi, A.; Hayat, T.; Pan, X.; Dai, S. Acquiring high-performance and stable mixed-dimensional perovskite solar cells by using a transition-metal-substituted Pb precursor. *ChemSusChem* **2018**, *11*, 3269–3275. doi:10.1002/cssc.201801171.
30. Ohishi, Y.; Oku, T.; Suzuki, A. Fabrication and characterization of perovskite-based $CH_3NH_3Pb_{1-x}GexI_3$, $CH_3NH_3Pb_{1-x}Tl_xI_3$ and $CH_3NH_3Pb_{1-x}In_xI_3$ photovoltaic devices. *AIP Conf. Proc.* **2016,** *1709*, 020020. dx.doi:10.1063/1.4941219.
31. Klug, M. T.; Osherov, A.; Haghighirad, A. A.; Stranks, S. D.; Brown, P. R.; Bai, S. et al. Tailoring metal halide perovskites through metal substitution: Influence on photovoltaic and material properties. *Energy Environ. Sci*. **2017,** *10*, 236–246. doi:10.1039/C6EE03201J.
32. Suzuki A.; Oe M.; Oku T., Fabrication and characterization of Ni-, Co-, and Rb-incorporated $CH_3NH_3PbI_3$ perovskite solar cells, *J. Electronic Mater.* **2021**, *50*, 1980-1995. Doi: 10.1007/s11664-021-08759-1.

33. Wang L.; Zhou H.; Hu J.; Huang B.; Sun M.; Dong B.; Zheng G.; Huang Y.; Chen Y.; Li L.; Xu Z.; Li N.; Liu Z.; Chen Q.; Sun L.D.; Yan C.H., A Eu^{3+}-Eu^{2+} ion redox shuttle imparts operational durability to Pb-I perovskite solar cells, *Science*, **2019**, *363*, 265-270. doi:10.1126/science.aau5701.
34. Park, B. W.; Philippe, B.; Zhang, X.; Rensmo, H.; Boschloo, G.; Johansson, E. M. J. Bismuth based hybrid perovskites $A_3Bi_2I_9$ (A: methylammonium or cesium) for solar cell application. *Adv. Mater.* **2015**, *27*, 6806–6813.
35. Ueoka, N.; Oku, T.; Suzuki, A.; Sakamoto, H.; Yamada, M.; Minami, S.; Miyauchi, S. Fabrication and characterization of CH_3NH_3(Cs)Pb(Sn)I_3(Cl) perovskite solar cells with TiO2 nanoparticle layers. *Jpn. J. Appl. Phys.* **2018**, *57*, 02CE03. doi:10.7567/JJAP.57.02CE03.
36. Suárez, I.; Vallés-Pelarda, M.; Gualdrón-Reyes, A. F.; Mora-Seró, I.; Ferrando, A.; Michinel, H. Outstanding nonlinear optical properties of methylammonium- and Cs-PbX_3 (X = Br, I, and Br–I) perovskites: Polycrystalline thin films and nanoparticles. APL Mater. **2019,** *7*, 041106. doi:10.1063/1.5090926.
37. Jung, M. H.; Rhim, S. H.; Moon, D. TiO_2/$RbPbI_3$ halide perovskite solar cells. *Sol. Energy Mater. Sol. Cells* **2017,** *172*, 44–54. doi:10.1016/j.solmat.2017.07.011
38. Machiba, H.; Oku, T.; Kishimoto, T.; Ueoka, N.; Suzuki, A. Fabrication and evaluation of K-doped $MA_{0.8}FA_{0.1}K_{0.1}PbI_3$(Cl) perovskite solar cells. *Chem. Phys. Lett.* **2019**, *730*, 117–123, doi:10.1016/j.cplett.2019.05.050.
39. Kandori, S.; Oku, T.; Nishi, K.; Kishimoto, T.; Ueoka, N.; Suzuki, A. Fabrication and characterization of potassium- and formamidinium-added perovskite solar cells. *J. Ceram. Soc. JPN.* **2020**, *128*, 805–811, doi:10.2109/jcersj2.20090.
40. Oku, T.; Kandori, S.; Taguchi, M.; Suzuki, A.; Okita, M.; Minami, S.; Fukunishi, S.; Tachikawa, T. Polysilane-inserted methylammonium lead iodide perovskite solar cells doped with formamidinium and potassium. *Energies* **2020**, *13*, 4776; doi:10.3390/en13184776.
41. Suzuki, A.; Kato, M.; Ueoka, N.; Oku, T. Additive effect of formamidinium chloride in methylammonium lead halide compound-based perovskite solar cells. *J. Electron. Mater.* **2019**, *48*, 3900–3907, doi:10.1007/s11664-019-07153-2.
42. Yang, W. S.; Noh, J. H.; Jeon, N. J.; Kim, Y. C.; Ryu, S.; Seo, J.; Seok, S. I. High-performance photovoltaic perovskite layers fabricatedthrough intramolecular exchange. Science **2015,** *348*, 1234–1237. doi:10.1126/science.aaa9272.
43. Hsu, H.L.; Chang, C.C.; Chen, C.P.; Jiang, B.H.; Jeng, R.J.; Cheng, C.H. High-performance and high-durability perovskite photovoltaic devices prepared using ethylammonium iodide as an additive. *J. Mater. Chem. A* **2015,** *3*, 9271–9277. doi:10.1039/C5TA01563D.
44. Nishi, K.; Oku, T.; Kishimoto, T.; Ueoka, N.; Suzuki, A. Photovoltaic characteristics of $CH_3NH_3PbI_3$ perovskite solar cells added with ethylammonium bromide and formamidinium iodide. *Coatings* **2020**, 10 410−1−10, doi:10.3390/coatings10040410.
45. Kishimoto, T.; Suzuki, A.; Ueoka, N.; Oku, T. Effects of guanidinium addition to $CH_3NH_3PbI_{3-x}Cl_x$ perovskite photovoltaic devices. *J. Ceram. Soc. Jpn.* **2019**, *127*, 491−497, doi:10.2109/jcersj2.18214.
46. Gao, L.; Li, X.; Lin, Y.; Fang, J.; Huang, S.; Spanopoulos, L.; Li, X.; Wang, Y.; Chen, L.; Yang, G.; Kanatzidis, G. M. Incorporated guanidinium expands the $CH_3NH_3PbI_3$ lattice and enhances photovoltaic performance. *ACS Appl. Mater. Interfaces* **2020**, *12*, 43885, doi:10.1021/acsami.0c14925.
47. Kishimoto, T.; Oku, T.; Suzuki, A.; Ueoka, N. Additive effects of guanidinium iodide on $CH_3NH_3PbI_3$ perovskite solar cells. *Phys. Status Solidi A* **2021**, 218, 2100396, doi:10.1002/pssa.202100396.
48. Miyasaka, T.; Kulkarni, A.; Kim, G.M.; Öz, S.; Jena, A.K. Perovskite solar cells: Can we go organic-free, lead-free, and dopant-free? *Adv. Energy Mater.* **2020**, *10*, 1902500, doi:10.1002/aenm.201902500.
49. Hoefler, S.F.; Trimmel, G.; Rath, T. Progress on lead-free metal halide perovskites for photovoltaic applications: A review. *Monatsh. Chem.* **2017**, *148*, 795–826, doi:10.1007/s00706-017-1933-9.
50. Qiu, L.; Ono, L. K.; Qi, Y. Advances and challenges to the commercialization of organic–inorganic halide perovskite solar cell technology. *Mater. Today Energy* **2018,** *7*, 169–189, doi:10.1016/j.mtener.2017.09.008.
51. Ando, Y.; Oku, T.; Ohishi., Y. Rietveld refinement of crystal structure of perovskite CH3NH3Pb(Sb)I3 solar cells. *Jpn. J. Appl. Phys.* **2018,** *57*, 02CE02.
52. Wei, H.; Du, M. H.; Stand, L.; Zhao, Z.; Shi, H.; Zhuravleva, M.; Melcher, C. L. Scintillation properties and electronic structures of the intrinsic and extrinsic mixed elpasolites $Cs_2NaRBr_3I_3$ (R = La, Y). *Phys. Rev.* **2016,** Appl. *5*, 024008, doi:10.1103/PhysRevApplied.5.024008.
53. Xiao, Z.; Meng, W.; Wang, J.; Mitzi, D. B.; Yan, Y. Searching for promising new perovskite-based photovoltaic absorbers: The importance of electronic dimensionality. *Mater. Horiz.* **2017,** *4*, 206–216, doi:10.1039/C6MH00519E.
54. Oku, T. Direct structure analysis of advanced nanomaterials by high-resolution electron microscopy. *Nanotech. Rev.* **2012,** *5*, 389–425, doi:10.1515/ntrev-2012-0018.
55. Oku, T. High-resolution electron microscopy and electron diffraction of perovskite-type superconducting copper oxides. *Nanotech. Rev.* **2014,** *3*, 413–444, doi:org/10.1515/ntrev-2014-0003.
56. Rodríguez-Romero, J., Clasen Hames, B.; Galar, P.; Fakharuddin, A. Suarez, I.; Schmidt-Mende, L.; et al. Tuning optical/electrical properties of 2D/3D perovskite by the inclusion of aromatic cation. *Phys. Chem. Chem. Phys.* **2018,** *20*, 30189–30199, doi:10.1039/C8CP06418K.
57. Lee, B., Stoumpos, C. C.; Zhou, N.; Hao, F.; Malliakas, C.; Yeh, C. Y.; et al. Air-stable molecular semiconducting iodosalts for solar cell applications: Cs_2SnI_6 as a hole conductor. *J. Am. Chem. Soc.* **2014**, *136*, 15379–15385, doi: 10.1021/ja508464w.
58. Maughan, A. E., Ganose, A. M.; Scanlon, D. O.; Neilson, J. R. Perspectives and design principles of vacancy-ordered double perovskite halide semiconductors. *Chem. Mater.* **2019,** *31*, 1184–1195, doi: 10.1021/acs.chemmater.8b05036.

59. Dai, W. B., Xu, S.; Zhou, J.; Hu, J.; Huang, K.; Xu, M. Lead-free, stable, and effective double $FA_4Ge^{II}Sb^{III}Cl_{12}$ perovskite for photovoltaic applications. *Sol. Energy Mater. Sol. Cells* **2019,** *192,* 40–146, doi:10.1016/j.solmat.2018.12.031.
60. Ju, M. G., Chen, M.; Zhou, Y.; Garces, H. F.; Dai, J.; Ma, L.; et al. Earth-abundant nontoxic titanium(IV)-based vacancy-ordered double perovskite halides with tunable 1.0 to 1.8 eV bandgaps for photovoltaic applications. *ACS Energy Lett.* **2018,** *3*, 297–304, doi: 10.1021/acsenergylett.7b01167.
61. Willett, R., Place, H.; Middleton, M. Crystal structures of three new copper(II) halide layered perovskites: Structural, crystallographic, and magnetic correlations. *J. Am. Chem. Soc.* **1988,** *110*, 8639–8650, doi:10.1021/ja00234a010.
62. Pabst, I.; Fuess, H.; Bats, J. W. Structure of monomethylammonium tetrachlorocuprate at 297 and 100 K. *Acta Crystallogr. C* **1987**, *43*, 413–416, doi:org/10.1107/S0108270187095568.
63. Mao, L.; Ke, W.; Pedesseau, L.; Wu, Y.; Katan, C.; Even, J.; et al. Hybrid Dion-Jacobson 2D lead iodide perovskites. *J. Am. Chem. Soc.* **2018,** *140*, 3775–3783.
64. Stoumpos, C. C.; Cao, D. H.; Clark, D. J.; Young, J.; Rondinelli, J. M.; Jang, J. I.; Hupp, J. T.; Kanatzidis M. G. Ruddlesden–Popper hybrid lead iodide perovskite 2D homologous semiconductors. *Chem. Mater.* **2016,** *28*, 2852–2867, doi:10.1021/acs.chemmater.6b00847.
65. Mao, L., Teicher, S. M. L.; Stoumpos, C. C.; Kennard, R. M.; DeCrescent, R. A.; Wu, G.; et al. Chemical and structural diversity of hybrid layered double perovskite halides. *J. Am. Chem. Soc.* **2019,** *141*, 19099–19109. doi:org/10.1021/jacs.9b09945.
66. Suzuki A.; Miyamoto Y.; Oku T., Electronic structures, spectroscopic properties, and thermodynamic characterization of sodium- or potassium-incorporated $CH_3NH_3PbI_3$ by first-principles calculation *J. Mater. Sci.* **2020**, *55*, 9728–9738. doi:10.1007/s10853-020-04511-y.
67. Suzuki A.; Oku T., Effects of mixed-valence states of Eu-doped $FAPbI_3$ perovskite crystals studied by first-principles calculation, *Mater. Adv.*, **2021**, *2*, 2609-2616, doi:10.1039/d0ma00994f.